AD-A268 629

Contract N00014-90-J-1392

Final Report
to
Office of Naval Research
Materials Division - Code 431 N
Arlington, VA 22217

DTIC
ELECTE
AUG 3 0 1993
S
E
D

INTERFACE CHEMISTRY IN CERAMIC MATRIX COMPOSITES

Department of Materials Science and Engineering
The Pennsylvania State University
University Park, PA 16802

March 1993

STRIBUTION STATEMENT A
Approved for public release;
Distribution Unlimited

93-20226

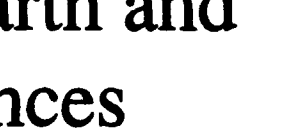

PENNSTATE

College of Earth and
Mineral Sciences

93 8 27 117

93 6 24 016

The Pennsylvania State University is committed to the policy that all persons shall have equal access to programs, facilities, admission, and employment without regard to personal characteristics not related to ability, performance, or qualifications as determined by University policy or by state or federal authorities. The Pennsylvania State University does not discriminate against any person because of age, ancestry, color, disability or handicap, national origin, race, religious creed, sex, sexual orientation, or veteran status. Direct all affirmative action inquiries to the Affirmative Action Office, The Pennsylvania State University, 201 Willard Building, University Park, PA 16802-2801. U.Ed. EMS 93-05

PREFACE

This report summarizes the work performed at The Pennsylvania State University during the period 1 January 1990 to 31 January 1993 under ONR Contract N00014-90-J-1392. The principal investigator was Professor Carlo G. Pantano; Professor Karl Spear and graduate students Greg Bibbo, Jim Walck, Anant Singh, Gang Qi and Doug Beall, were co-investigators. The following is a complete list of publications for the 1990-1993 period.

LIST OF PUBLICATIONS

Interface Reaction and Wetting in Carbon Fiber Reinforced Glass Matrix Composites
C. G. Pantano, G. Chen and D. Qi
Mat. Sci. and Eng., A126, 191 (1990).

Sol/Gel Processing and Crystallization of Yttrium-Aluminosilicate Glasses
J. Walck and C. G. Pantano
J. Non-Crystal. Sol., 124, 145 (1990).

The Effect of Carbon Monoxide Partial Pressure on the High Temperature Decomposition of Nicalon Fiber
G. S. Bibbo, P. M. Benson, and C. G. Pantano
J. Mat. Sci., 26, 5075 (1991).

Sol/Gel Processing of Oxycarbide Glasses and Glass Matrix Composites
H. Zhang and C. G. Pantano
in Ultrastructure Processing of Advanced Materials, D. Uhlmann and D. Ulrich, Editors
(Wiley, New York, 1992) pp. 223-233.

Effects of Composite Processing on the Performance of Carbon Fiber/Glass Matrix Composites
D. Qi and C. G. Pantano
Ceram. Eng. and Sci. Proc., 13, 863 (1992).

Sol-Gel Prepared Ni-Alumina Composite Materials
Part I. Microstructure and Mechanical Properties,
E. Breval, Z. Deng, S. Chiou and C. G. Pantano
J. Mater. Sci., 27, 1464 (1992).

Sol-Gel Prepared Ni-Alumina Composite Materials
Part II. Structure and Hot-Pressing Temperature
E. Breval and C. G. Pantano
J. Mater. Sci., 27, 5463 (1992).

The Role of Si-H Functionality in Oxycarbide Glass Synthesis
A. K. Singh and C. G. Pantano
MRS Symp. Proc., 271, 795 (1992).

Carbon-Layer Formation at Silicon-Carbide/Glass Interfaces
G. Qi, K. E. Spear and C. G. Pantano
Materials Science and Engineering (to appear in 1993).

Interface Reactions in Glass Matrix Composites
C. G. Pantano, K. E. Spear, G. Qi and D. Beall
Ceramic Transitions (to appear in 1993).

Accesion For	
NTIS CRA&I	☒
DTIC TAB	☐
Unannounced	☐
Justification	
By	
Distribution /	
Availability Codes	
Dist	Avail and / or Special
A-1	

DTIC QUALITY INSPECTED 3

TABLE OF CONTENTS

INTRODUCTION

There are many possible effects of interface reactions in fiber or whisker reinforced glass or glass ceramic matrix composites. In most cases, interface reactions must be minimized because they can lead to degradation of fiber or whisker strength, destruction of interphase coatings, and modification of the interface adhesion. Nevertheless, there are systems where interface reactions are beneficial. The best example of this is in the NiCALON reinforced glass-ceramic composites where carbon interphases are generated during processing; this carbon interphase facilitates fiber pullout, and thereby, is responsible for the outstanding room-temperature toughness of these materials. (1,2) There have also been suggestions, although less well documented, that interface reactions can create carbide, nitride and mullite interphases that passivate the interface to subsequent oxidation. (3,4)

In general, a fundamental understanding of interface reactions—during processing and service—is still in the development stages. This is especially true in the case where multicomponent glass matrix composites are employed. Although the formalisms required for thermochemical calculations of local equilibrium and reaction kinetics have been developed (5,6), the thermodynamic and transport properties necessary to model and predict evolution of the interface in multicomponent systems are simply not available.

Here, some of the most important interface reactions in non-oxide reinforced multicomponent glass matrix systems will be reviewed. It will be demonstrated that in many cases, simple thermochemical models of glass solutions are sufficient to establish the driving forces for the reactions. This is true even in the case of the non-stoichiometric carboxide and carbonitride reinforcement phases. On the other hand, the transport properties of various constituents, and the solubility of gaseous reaction products, must be approximated or deduced from experimental data. Fortunately, there is now a wide spectrum of data and observations in the literature about specific interactions at fiber/matrix interfaces (1-4, 7-10). Subsequently, a kinetic model that predicts the extent of carbon interphase formation at SiC/glass interfaces will be described, and then used to design the processing parameters in a model composite fabrication. Some

experimental data is presented to verify the predictions. The discussions and examples are focused on SiC reinforcement phases, but the phenomenology can be extended to include nitride and carbonitride reinforcement phases.

THERMOCHEMISTRY

In the absence of an external oxidizing or reducing atmosphere, redox interactions between the reinforcement phase (including a surface oxide or coating), and the matrix glass solution, are of primary concern. These redox interactions are of practical relevance during processing of the composite; since this fabrication is most often performed in an inert atmosphere or vacuum hot-press, and are intrinsic to the composition of the reinforcement and matrix. These reactions are also relevant to the high temperature performance of a composite in an inert environment, or in any environment where transport of external reactants to the interface is limited.

There are two important redox interactions to be considered. One of these concerns variable valence oxides present in the glass:

$$M_xO_y \leftrightarrow M_xO_{y-2} + O_2 \qquad (1)$$

The oxide M_xO_y represents a source (or sink) for oxygen at the interface of composites. The extent to which it may provide or consume oxygen depends upon the specific metal oxide in question; this is typically represented in terms of a temperature dependent free-energy value or P_{O_2}. Figure 1 presents plots of the equilibrium P_{O_2} values for the most common oxides used in glasses. Some of these compounds may provide oxygen through a valence change (Figure 1a), while others must be reduced to the metallic state (Figure 1b). In general, most glass-forming constituents prefer the oxide state, and are reduced only at very low P_{O_2}. The higher equilibrium P_{O_2}'s associated with the As- and Sb- oxides is most obvious; these are often used as fining agents in glass. It is also evident that Fe_2O_3 exhibits a high P_{O_2}; it is a common impurity in commercial glasses.

The more relevant situation, of course, concerns glass solutions wherein mixtures of various oxides (M_xO_y) must be considered. Here, the state of equilibrium of M_xO_y (i.e., reaction (1)) will be determined by the composition of

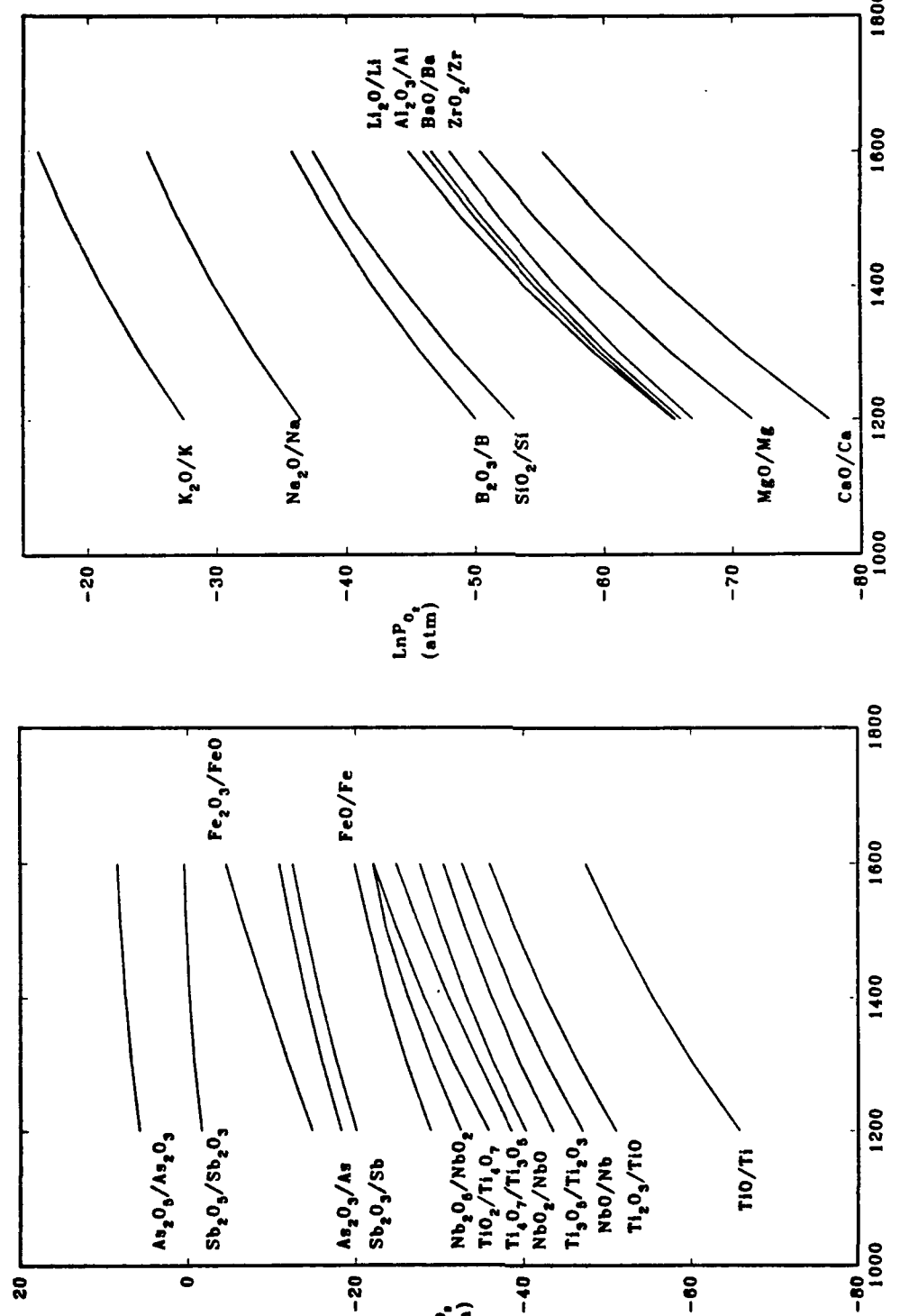

Figure 1. The equilibrium oxygen partial pressures for the most common oxides used in glass.

the glass and the melting history. The glass solution, itself, does not exert a strong influence upon the redox potential. Usually, oxide-oxide associations in compounds and solutions lower the activity of each oxide, and thereby lower each respective oxide decomposition pressure, but the binding energy of oxygen to a metal is relatively independent of these associations. Thus, the relative order in which several metal oxides in a glass would be reduced does not change from the order with which the pure oxides would be reduced. The only exception to this occurs when pure oxides exhibit similar oxygen pressures, and their concentrations in the glass solution are quite different.

The specific dependence of oxide activities on glass composition is calculated by using a thermodynamic description developed by Hastie and co-workers (11) for representing multicomponent MHD oxide slags. This description was used previously to model interface reactions in carbon-fiber reinforced glass matrix composites (12). The excess mixing energy in the model is included through the use of *associate liquid species* with known formation energies. These *associate liquid species* fix the free energy of formation for specific chemical compositions of the glass. The model does not imply that identifiable associate species are present in the glass phase, but the tendency of various oxides to associate at specific compositions is represented by the formation energies of the associate species. This solution model provides the best known thermodynamic representation for complex multicomponent glass phases. These calculations are carried-out using the computer-code termed ChemSage (13).

The effect of glass composition and melting history can be quite significant when variable valence oxides are present. The variable valence oxide can provide an internal source of oxygen in the composite; if the glass frit used to fabricate the composite is melted in air, the oxide equilibria can be very different than if it is melted in vacuum. Consider the situation where a multicomponent glass (M_xO_y·CaO·Al_2O_3·SiO_2) is melted in air (P_{O_2} = .21) vs vacuum ($P_{O_2} \approx 10^{-10}$). There will be negligible effects of the melting atmosphere upon the Ca, Al and Si oxides. But there can be a substantial difference in the M_xO_y to M_xO_{y-2} ratio

quenched into the glass (see reaction 1). During composite fabrication, the (local) equilibrium P_{O_2} at the non-oxide/matrix interface will be determined by this ratio. Since the equilibrium P_{O_2} at the SiC/oxide interface is quite low ($\sim 10^{-19}$), there is always a driving force for reducing the oxygen activity in the glass by oxidizing the non-oxide reinforcement. The extent of this reaction will be much greater in the case of the glass melted in air because the higher activity of M_xO_y creates a large source of oxygen near the interface. This is one mechanism through which glass composition and melting history plays a role in the interface reaction. In the absence of M_xO_y in the glass formulation, this reaction and dependence upon melting history could be eliminated. (There may also exist a quenched-in oxygen activity due solely to the molecular solubility of O_2 in the melt, but this effect cannot be described quantitatively; moreover, it is probably negligible).

Of course, it is the ability to control and predict the local oxygen content and activity within the matrix that is of interest. Figure 2 shows, for example, the relationship between oxygen activity, temperature and melting history for a lithium-aluminosilicate glass containing 1% As_2O_{3+x}. The P_{O_2} maintained during melting and quenching will fix the As_2O_5 to As_2O_3 ratio in the glass. During composite fabrication in a non-oxidizing environment, the glass will exhibit an oxygen activity (or, equivalently, will create a local P_{O_2}) determined by the As_2O_5/As_2O_3 ratio. Since some oxidation may be required for in-situ formation of carbon interphases (see below), tailoring of the interfacial P_{O_2} may be required in the fabrication stage. In this sense, the reproducibility and reliability of the composite fabrication process depends upon melting history, and perhaps of greater importance, (variable valence) impurity content. The most common impurities in glasses are transition metal oxides and water, and while all of these have not been included in Figure 1, their redox potential is in the range of the As, Sb, Nb, Fe and Ti oxides. Thus, even low concentrations may yield substantial interface effects.

The other, perhaps more important, redox interactions in glass matrix composites are the reactions between non-oxide reinforcement phases (SiC and C

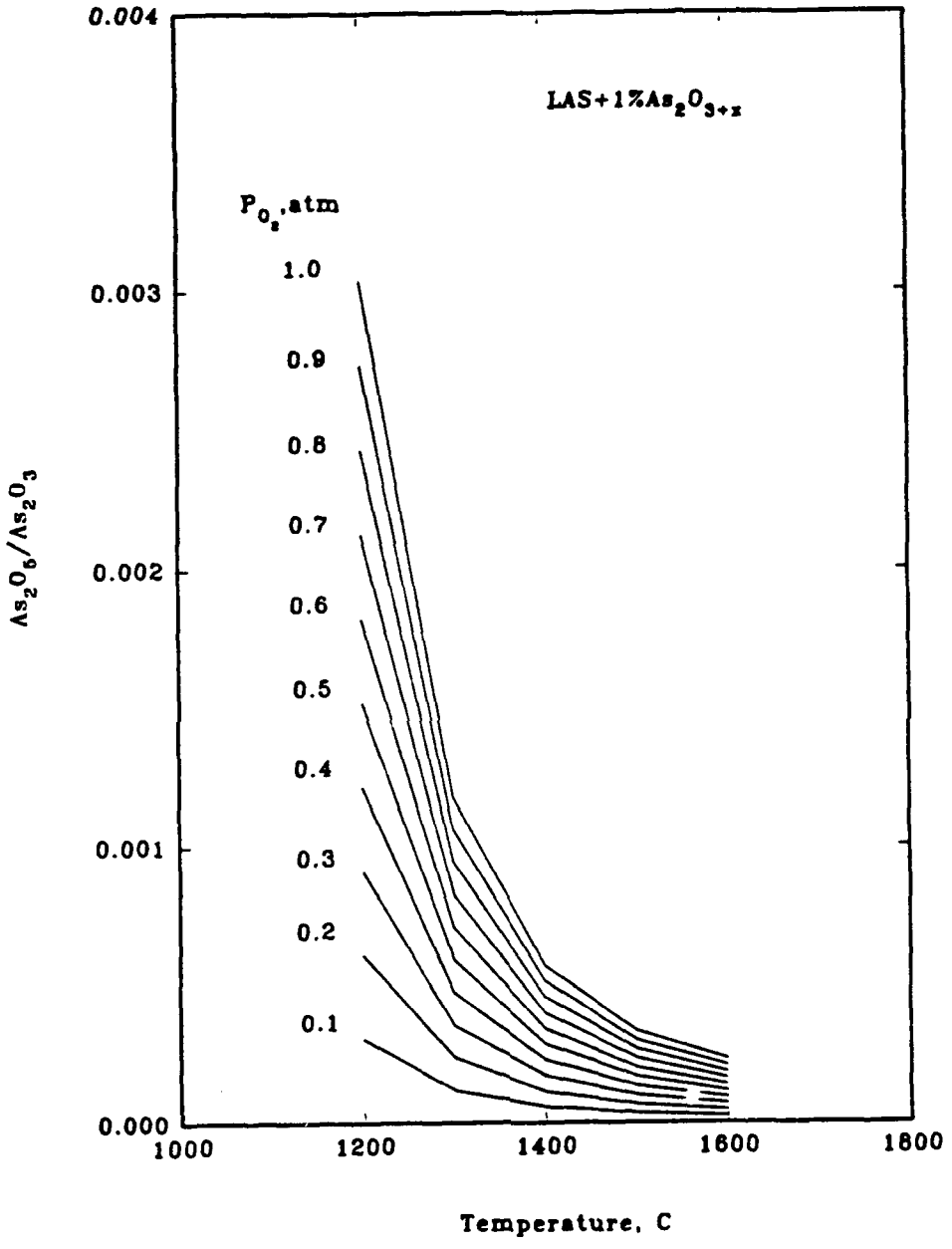

Figure 2. The effect of oxygen activity during melting and quenching upon the As_2O_5/As_2O_3 ratio in an LAS glass; or equivalently, the effect of this ratio upon the initial oxygen activity of the glass upon heating.

in this case) and specific oxides in the matrix. The glass composition and melting history define the driving forces for these reactions:

$$M_xO_y + SiC = M_xO_{y-2} + SiO_2 + C \quad (2a)$$

$$M_xO_y + SiC = xM + SiO_2 + CO_y + SiO_2 + C \quad (2b)$$

$$Glass + SiC = Glass' + C \quad (2c)$$

Glass' represents the glass solution phase whose oxygen activity and composition have been influenced by the reaction with SiC (e.g., a solution of SiO_2, M_xO_y, M and *Glass*). It is also important to recognize that gaseous reaction products, primarily CO, can have high activities in this three-phase equilibrium (Glass, SiC, C), but for the purposes of these thermochemical calculations, the gas volume is fixed at zero to model the interface. Thus, the calculated equilibrium pressures of gaseous reaction products represent thermodynamic activities which provide a driving force for the reaction.

The effect of glass composition upon reaction (2) can be evaluated in a number of ways. Figure 3 represents the extent of reaction with SiC in terms of the production of carbon. This is relevant to the formation and stability of carbon interphases during composite fabrication. It can be seen that some of the oxides (B, Ba, Ca, Li, Nb and Zr) do not yield any carbon because their respective metal - carbides are more stable than carbon. In these calculations, the activity of SiC has been fixed at 1; i.e., there is an abundance of SiC in the system. Also, the SiO_2 product from the oxidation of the SiC is assumed to form a solution phase with the metal oxide species. Therefore, Figure 3 also reveals the extent to which the various oxides might degrade the surface of a SiC reinforcement phase through oxidation. In fact, the moles of carbon (or metal-carbide) produced are quantitatively equal to the moles of SiC consumed (see Reaction 2). Clearly, they scale roughly with the equilibrium P_{O_2}'s shown in Figure 1.

Figure 4 describes the stability of the C (generated in reaction 2) in terms of the local CO pressure:

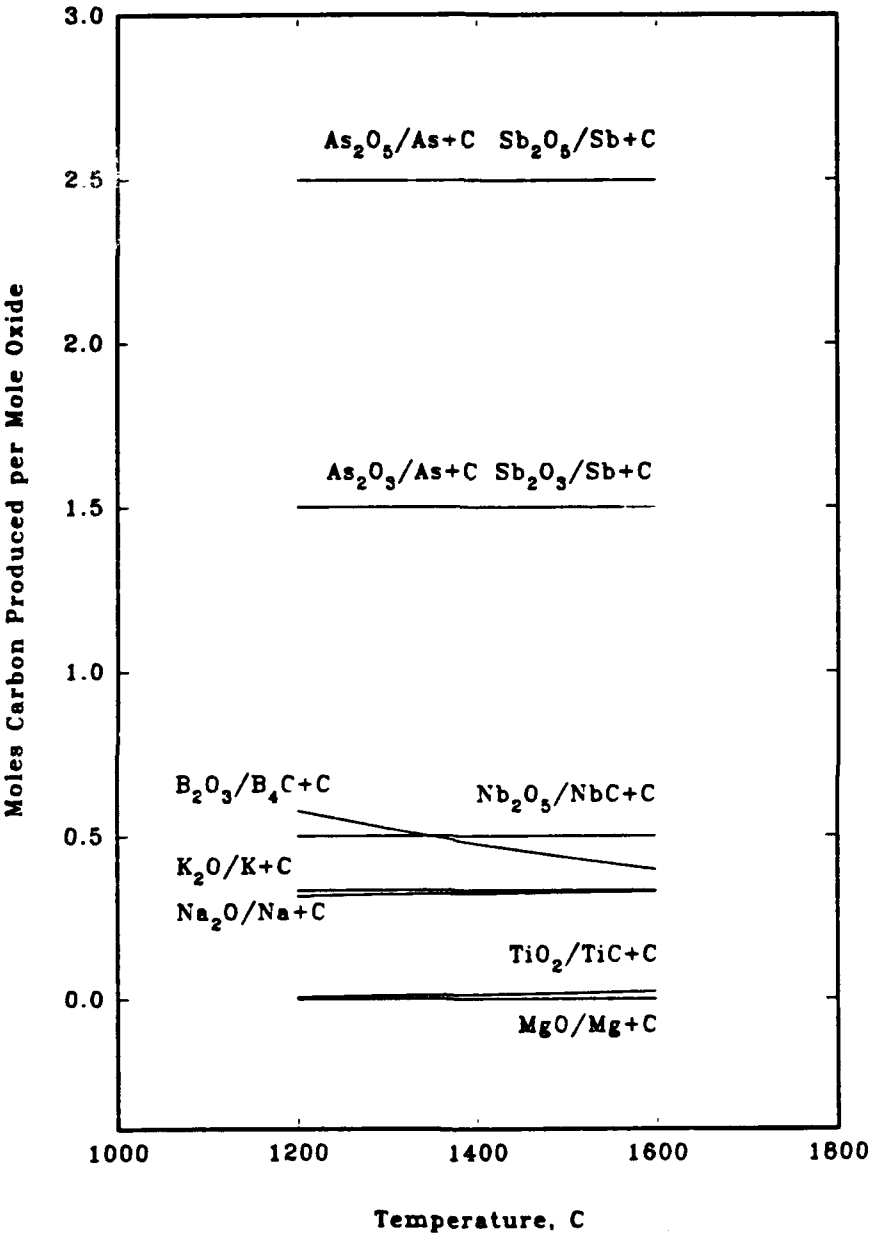

Figure 3. The moles of carbon produced per mole of oxide during the reaction of various oxides with (excess) SiC; the oxides NbO, BaO, Li_2O, CaO and ZrO_2 react to form metal carbides in preference to carbon.

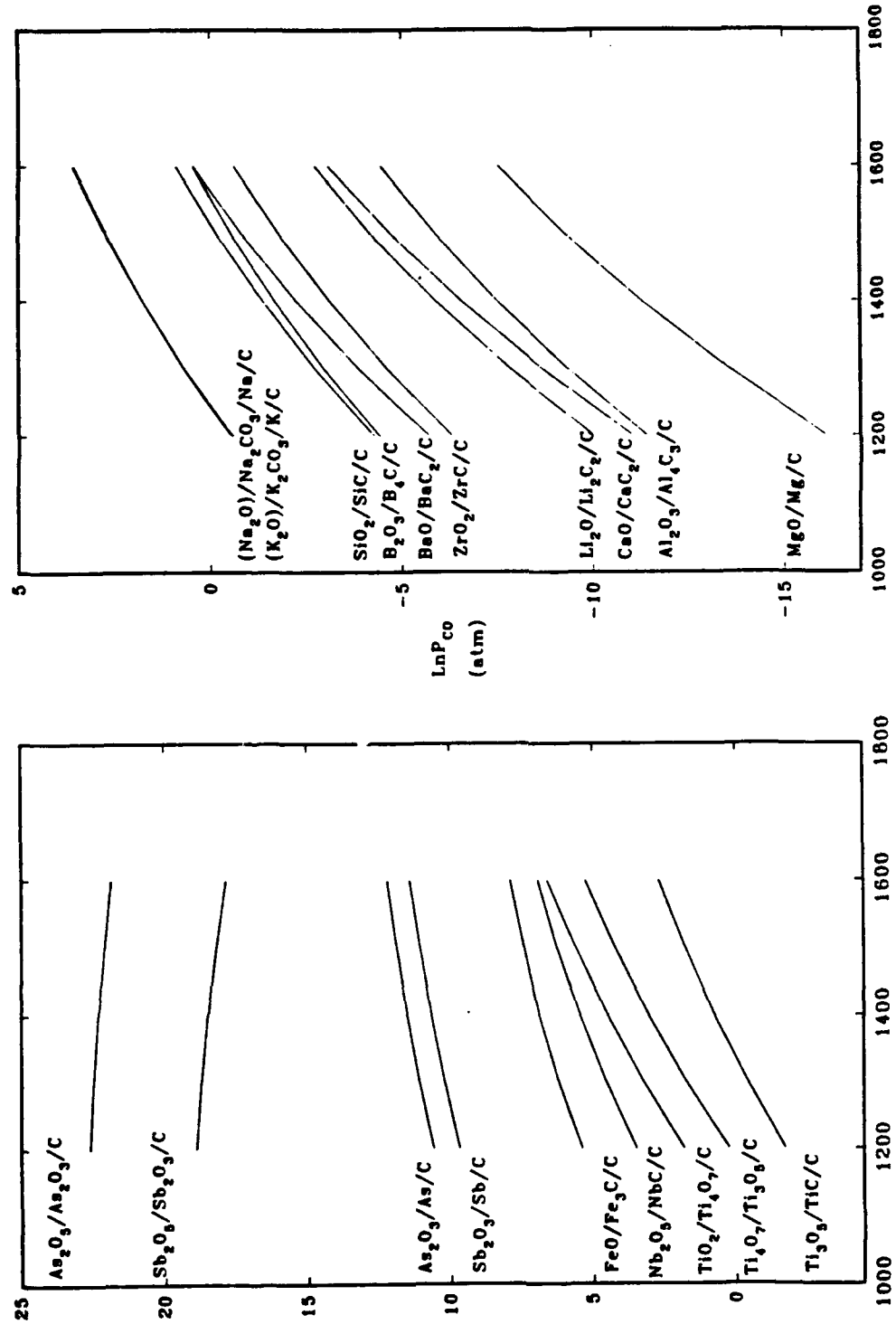

Figure 4. The CO pressure (at near zero gas volume) required to maintain equilibrium between carbon, various metal oxides and the product of their reduction.

$$M_xO_y + 2C = M_xO_{y-2} + 2\,CO. \qquad (3)$$

In Figure 4, the SiC and C activities are fixed at 1; that is, SiC and C are assumed to exist in the system even in the case where metal carbides may also be present. The pressures are very high because the gas volume has been constrained to zero. In general, it shows that the co-existence of SiC, C and oxide demands very high local CO activity in the case of those oxides where carbon formation via oxidation of SiC is most probable. This plot can be interpreted and used in a variety of ways. It implies a strong tendency for bubble formation at the interface in those systems with high P_{CO}. Similarly, it reveals that carbon coatings applied to fibers and exposed to oxides with high equilibium P_{CO} will be rapidly degraded. It can also be concluded that the oxide species with low P_{CO} will not react extensively with carbon coatings. And in the absence of an applied carbon coating, their limited redox reaction with SiC will not provide any driving force for in-situ carbon interphase formation (see Figure 3).

The calculations in Figures 3 and 4 consider only the pure oxides and their solutions with the SiO_2 reaction product (Reactions 2a and 2b). These have been presented to illustrate the effects of specific oxides. In reality, though, the glass solutions, Reaction 2c, should be accounted for in the thermochemical modeling of this oxidation reaction; this is important where variable valence oxides are present in the glass (Figure 2). In general, it is Reaction 2c that is used to model interface reactions with glass matrices, and it is the effective P_{O_2} of the *glass* that determines the driving force for the reaction. The calculations used for the kinetic modeling of carbon interphase formations do, in fact, include this effect (see next section).

KINETIC MODEL OF IN-SITU CARBON INTERPHASE FORMATION

The interface reactions in multicomponent systems are very complicated, and although thermodynamic approaches can provide insight to the local state of equilibrium and the driving force for reaction, the kinetics of transport are fundamental to the mechanisms and morphology of the reaction product. The lack of transport and solubility data for the glass solution phase precludes the

presentation of a mechanistic model at this time. But, the basic thermochemistry presented in the last section can be used to develop a phenomenological model that qualitatively describes the amount of carbon available at the interface for carbon layer formation. Although this model considers only the effect of oxidation in carbon formation (reaction 2), and it assumes stoichiometric SiC rather than the more reactive SiO_xC_y polymer-derived fibers (NiCALON), it successfully explains many of the observations in NiCALON-reinforced glass composites. (A more detailed description of this model is presented elsewhere (14)).

The reactions (2) and (3) show that silicon carbide (SiC) and oxygen (O_2) are consumed by the formation of C, SiO_2 and CO. According to the mass conservation principle, there is an oxygen balance at the interface such that:

$$n_{O_2} = n_{SiO_2} + 1/2\, n_{CO} \tag{4}$$

where n = number of moles per unit area. Because carbon is a product of SiC oxidation, the total carbon yield should be equal to the silica yield on a molar basis. But carbon may subsequently be oxidized to form CO. Therefore, the carbon balance is:

$$\begin{aligned} n_C{}^i &= n_{C\ total} - n_{CO} \\ &= n_{SiO_2} - n_{CO} \\ &= n_{O_2} - 3/2 n_{CO}, \end{aligned} \tag{5}$$

where $n_C{}^i$ is the moles of carbon at the interface per unit area and $n_{C\ total}$ = moles of carbon per unit area due to SiC oxidation. The moles of reactant (O_2) and reaction product (CO) can be represented by their flux, J, in or out of the interface. The flux, J, is simply the number of moles per unit area per unit time, and so equation (5) can be rewritten

$$n_C{}^i = \int J_{O_2}\, dt - 3/2 \int J_{CO} dt \tag{6}$$

Equation (6) is the basis of this interface reaction model for carbon-layer formation. In general, it should yield the time and temperature dependence of carbon layer mass (or thickness, assuming some value of density).

The driving force for O_2 diffusion from the glass to the interface can be represented by the chemical potential (μ), or concentration (c), of O_2. According to Darken's equation,

$$J_{O_2} = (-D_{O_2}^*/RT)C_{O_2}\, d\mu/dx$$
$$= D_{O_2}^* C_{O_2} (\ln P_{O_2}^g - \ln P_{O_2}^i)/X \qquad (7)$$

where $D^*_{O_2}$ is the self-diffusion coefficient of O_2, and $P_{O_2}^g$ and $P_{O_2}^i$ are the oxygen activities in the glass and at the interface, respectively. Since the oxygen comes from the glass itself, the concentration near the interface will decrease with time. Figure 5 shows, schematically, how this local oxygen depletion is modeled. If the interface is planar, the position (X) where the concentration does not change is simply:

$$X = 5.6\sqrt{(D_{O_2}t)} \qquad (8)$$

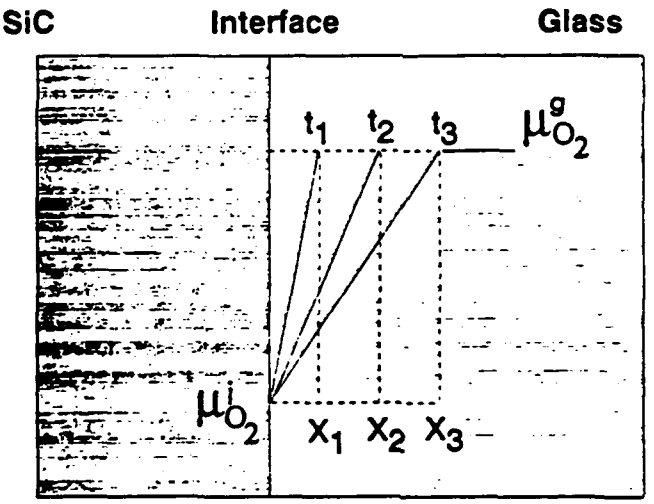

Figure 5. Schematic representation of the time-dependent decrease in chemical potential of oxygen near the SiC/glass interface.

The average concentration of oxygen in the glass, C_{O_2}, determines how much oxygen can be supplied by the glass. If the chemical potential is assumed to be linear with distance, the corresponding concentration would be an exponential function of distance X. Thus, the average concentration can be given by:

$$C_{O_2} = (C_{O_2}^{g} - C_{O_2}^{i})/(\ln C_{O_2}^{g} - \ln C_{O_2}^{i}) \qquad (9)$$

Altogether, then, the oxygen flux at a planar interface is

$$J_{O_2} = D^*_{O_2}[(C_{O_2}^{g} - C_{O_2}^{i})/(\ln C_{O_2}^{g} - \ln C_{O_2}^{i})]\ (\ln P_{O_2}^{g} - \mathrm{Ln} P_{O_2}^{i})/5.6\sqrt{(D_{O_2} t)} \qquad (10)$$

The oxygen concentrations and pressures in equation (10) are calculated using the thermochemical approaches described in the last section.

An important difference between surface oxidation and the interface reaction in composites, is that the out-diffusion distance for CO is not equal to the in-diffusion distance for O_2 (X in equation 4). In this case, the glass matrix thickness, L, is used to denote the CO out-diffusion distance; thus,

$$J_{CO} = D_{CO} C_{CO}^{i}/L \qquad (11)$$

The concentration of CO at the interface (C_{CO}^{i}) depends on the O_2 flux and the solubility of CO in the glass. Initially, reaction (2) will dominate the interface reaction mechanism. Later, the activity of SiC at the interface will decrease (due to the formation of C) and reaction (3) will compete with reaction (2). The CO concentration is related to the equilibrium CO pressure (P_{CO}^{i}) through the solubility constant, K; i.e.,

$$C_{CO}^{i} = K P_{CO}^{i} \qquad (12)$$

Since there is limited data for the solubility of CO in glasses, the constant K was calculated for SiO_2 using SiC single crystal oxidation rate data (K = .031). Since the solubility of CO in glasses is purely physical, it is unlikely that K is very sensitive to the composition.

Finally, then, the kinetics of carbon layer formation can be obtained by substituting the flux equations for O_2 and CO into equation (6):

$$n_C{}^i = \int J_{O_2}\,dt - 3/2 \int J_{CO}\,dt$$

$$= D^*O_2[(Co_2{}^g - Co_2{}^i)/(\ln Co_2{}^g - \ln Co_2{}^i)](\ln Po_2{}^g - \ln Po_2{}^i)/2.8\sqrt{t/Do_2{}^*}$$

$$- 3/2\, D_{CO}\, C_{CO}{}^i/L \qquad (13)$$

where D_{CO} is equal to $D^*O_2 = 92 \exp(56200/RT)$. The matrix thickness, L, has little effect provided that it is much greater than the oxygen depletion range ($5.6\sqrt{(D_{O_2}t)}$; here it was set equal to .5cm.

The concentrations and pressures in equation (13) are obtained using the ChemSage program. The ChemSage program is used, first, to calculate the oxygen activity in the glass, which depends upon the glass composition, melting temperature and melting atmosphere. In these calculations, a lithium - aluminosilicate composition (Corning Code 1723) was assumed but with variable amounts of arsenic oxide added. In most cases, the glasses were equilibrated with a $P_{O_2} = .21$ to simulate melting in air. The melting temperature was varied to further change the oxygen activity of the glass. The ChemSage program is used, subsequently, to calculate the interface concentrations and pressures between the glass and SiC.

Figures 6, 7 and 8 are calculations of the carbon layer thickness as a function of hot-pressing temperature and the oxygen activity (influenced by the % As_2O_{3+x}). In all cases, the moles of carbon calculated using equation 13 have been converted to an equivalent thickness of carbon-interphase. The density of the carbon interphase is experimentally found to be quite variable, but for the purposes of these calculations, a density value of $1.6 g/cm^3$ is used throughout.

Figure 6 shows the effect of the hot-pressing temperature upon the carbon layer formation. In all cases, the carbon interphase increases in thickness, and then decreases. (The decrease in carbon layer thickness is not within the time-frame of the plot for the 1100 and 1200°C calculations, but in fact, it does decrease at longer times). The increase in thickness is due to the initially higher O_2 flux relative to the CO flux. With time, however, the oxygen in the glass near

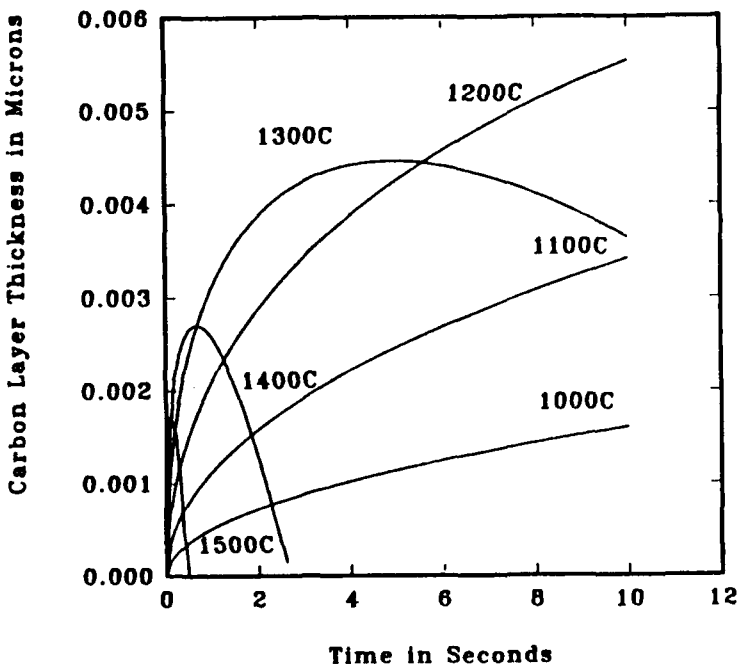

Figure 6

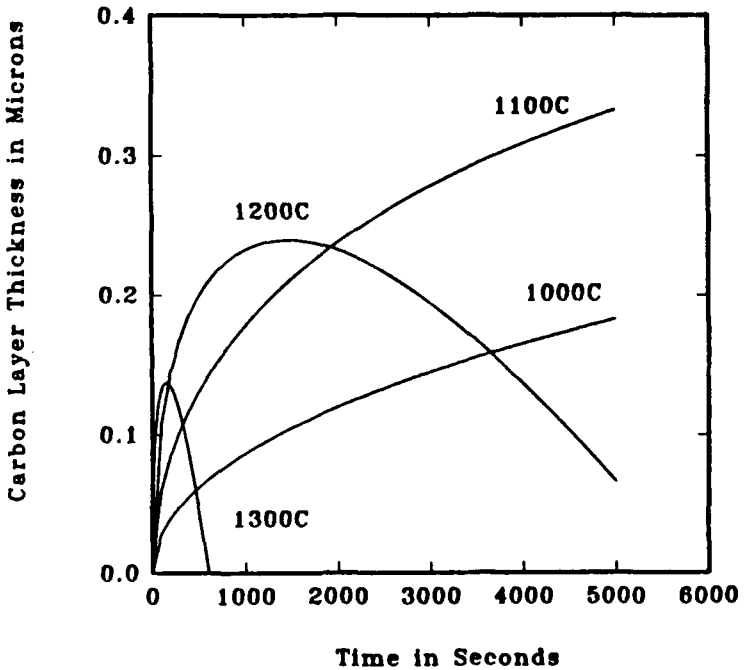

Figure 7

The carbon interphase thickness (at the glass/SiC interface) as a function of time for different hot-pressing temperatures; the LAS glass (with 1% As_2O_{3+x}) was initially equilibrated at 1400°C in Figure 6 and at 1200°C in Figure 7 with P_{O_2} = .21 to simulate melting and quenching in air.

the interface is depleted, and so, the O_2 flux decreases relative to the CO flux. Thus, the carbon interphase is consumed. Clearly, the transients are more rapid with increasing hot-pressing temperature.

Figure 7 shows an analogous plot of carbon layer formation, but for a glass initially equilibrated with air at 1200°C (in practice, LAS will crystallize if equilibrated at 1200°C, but for the purposes of this demonstration, thermochemical calculations of the As_2O_3/As_2O_5 equilibria were performed assuming the glassy state). It can be seen that the kinetics of carbon formation are most sensitive to the melting temperature when the hot-pressing temperature exceeds the melting temperature. This is due to the higher oxygen activity of the glasses melted at lower temperatures; i.e., the As_2O_3/As_2O_5 equilibria is shifted to As_2O_5 with a decrease in the melting temperature. Since these calculations assume that the equilibria at T_{melt} is quenched-in, they underestimate the effect. In fact, the melt can maintain equilibrium to lower temperatures (during cooling), and thereby, exhibit an even higher oxygen potential. It is to be emphasized that any variable valence oxide addition, or impurity in the glass, will exhibit this effect. This sensitivity of the interface reactions to the melting temperature depends upon the specific oxide and the melting atmosphere; in principle, it can be eliminated by melting in vacuum or at low P_{O_2}.

Figure 8 shows how the concentration of variable valence oxides influences the kinetics of carbon layer formation. The glass with the highest percentage of As_2O_3 shows the broadest range of stability for the carbon interphase. In general, though, the range of stability will depend upon the melting and hot-pressing temperatures. The calculations in Figure 8 assume melting and hot-pressing at 1200°C. Obviously, if the variable valence oxides are completely reduced, or eliminated in the glass composition, the model will calculate $n_C^i = O$. The thermochemical calculations (in ChemSage) do consider the possible reduction of major constituents in the glass (Li_2O, Al_2O_3 and SiO_2), but the activity of these reduced species is negligible. In reality, of course, there may be other sources of active oxygen or reducible oxides in glasses due to quenched-in gases and impurities.

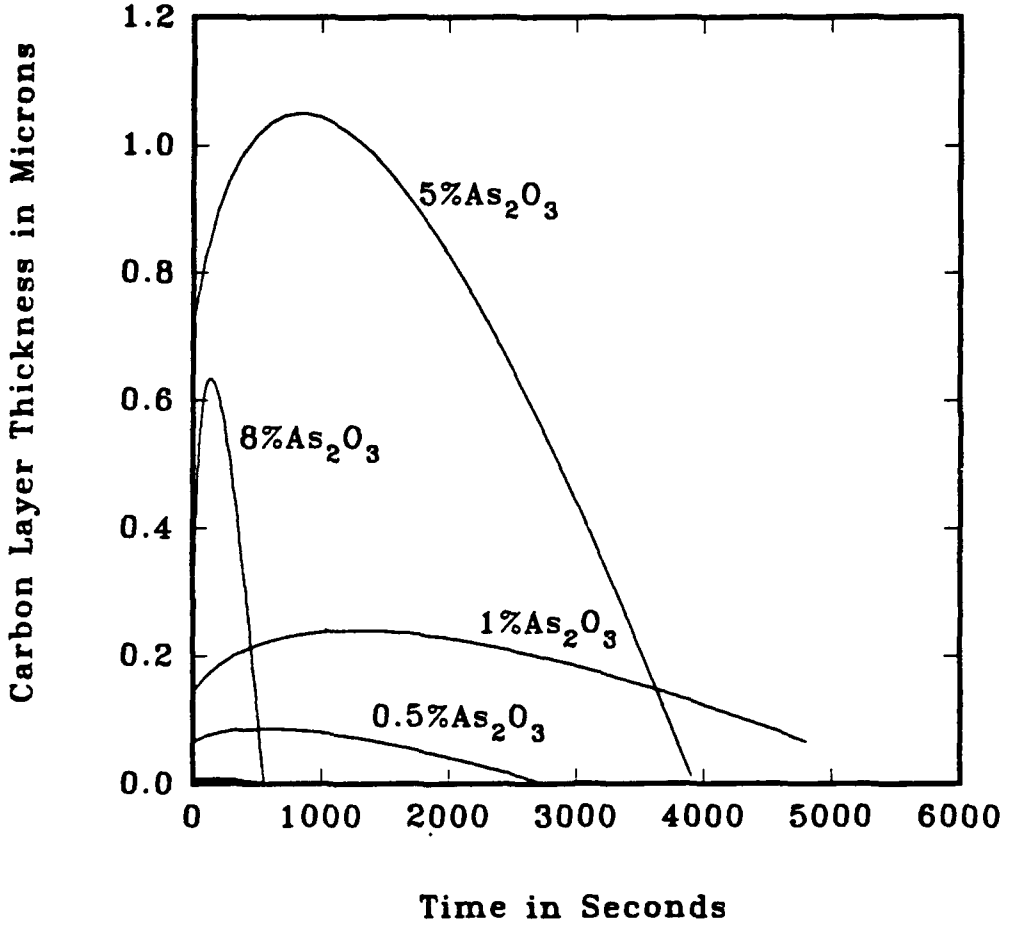

Figure 8. The carbon interphase thickness as a function of time for various glass compositions (or equivalently, for various local oxygen activities at the glass/SiC interface); the interface reactions were all at 1400°C, the glasses were all equilibrated at 1200°C with P_{O_2} = .21 to simulate melting and quenching in air, and the reactions (hot-pressing) were also at 1200°C.

It should be quite evident that the carbon layer thickness is transient in nature and varies considerably with the process parameters used in glass melting and composite fabrication. This probably accounts for the widely varying behavior of composites, the distribution of carbon layer thicknesses reported in the literature, and the extreme sensitivity of the composite toughness to the hot-pressing time. At the same time, it should also be evident that an equivalent thickness of carbon interphase can be created for very different conditions of processing or glass composition. However, this does not necessarily mean that the composite performance will be equivalent. In fact, experimental data [1-4, 7-10] shows that the mechanical properties of composites may be very different even if their carbon layer thicknesses are equal. This observation can be rationalized with this model, too, by examining the amount of SiO_2 formation that accompanies carbon layer formation. Obviously, there is a continuous increase in the amount of silica created, even though the carbon layer may be disappearing (due to the CO out-diffusion flux exceeding the O_2 flux at the interface). The amount of silica formation represents the extent of SiC oxidation, and in this sense, is a measure of the fiber degradation.

NiCALON FIBER/GLASS MATRIX COMPOSITES

The objective of these experiments was to determine whether the oxygen potential of a glass would, in fact, affect the interface reactions which occur during composite processing in a hot press where the external oxygen pressure is very low; that is, some model composites were fabricated to test the predictions of the model. In this study, the nominal glass composition was held constant, but the melts were prepared in closed crucibles wherein the oxygen activity was varied. Otherwise, the composite processing conditions and NiCALON fiber reinforcements were fixed. The mechanical and interfacial properties of these composites are described here.

A series of melts of Corning Code 7740 sodium boroaluminosilicate (Pyrex) glasses were made. A *standard* 7740 melt was prepared with the usual batch materials by melting in air at 1600°C. An *oxidized* melt was prepared (but in a closed crucible) with the substitution of sodium-sulfate for the usual sodium-

carbonate. And a *reduced* melt was prepared (also in a closed crucible) with the addition of sugar (dextrose) to the usual batch. The cast glasses were ball milled to produce frit, and then uniaxial prepregs were fabricated by the slurry infiltration technique. The prepregs were stacked and hot pressed at 1080°C (corresponding to a viscosity of approximately 10^5 poise) and 500 psi for 30 minutes.

The flexural strengths of the composites were determined by the 4-point bend test. The average strength values for the 3 different composites are given in Table 1. It can be seen that the strength of the composite with the *reduced* glass was greater than the other two by more than a factor of two. The mode of fracture was also quite different. The fracture plane in the composites made with the standard and oxidized glasses was typically perpendicular to the fiber direction and showed little or no sign of fiber pullout. In the composite made with the *reduced* glass, a considerable amount of fiber pullout was observed and the fracture plane was deflected down the axis of the fibers. These observations verify that the melting history of the glass matrix precursors can influence the final composite properties.

Table 1. Influence of the glass matrix phase upon the mechanical behavior of NiCALON reinforced glass composites

Melting history of glass frit →	strongly oxidizing	oxidizing	reducing
Flexural strength (MPa) →	180	230	520
Fiber pullout →	no	no	yes

Notes: (1) all glasses were melted 16 hours @ 1600°C
(2) 40 volume percent fibers
(3) composites hot-pressed at 10^5p (1080°C) and 500 psi
(4) glass composition = 81 SiO_2, 13 B_2O_3, Na_2O, 2 Al_2O_3 (by weight)

Figures 9a and 9b compare the scanning Auger depth-profiles of NiCALON fiber pull-outs in the *reduced*-matrix and *oxidized*-matrix composites. The presence of a carbon-rich interphase is clearly evident in the case of the *reduced*-matrix composite. This most certainly explains its superior mechanical properties. Nevertheless, it can be noted that boron has penetrated the fiber surface/interphase. This indicates that a reaction has, in fact, occurred between the fiber and matrix. On the other hand, the *oxidized*-matrix composite does not show a distinct carbon-layer at the interface. Moreover, the boron profile extends beyond the 2000Å range of the analysis. This suggests considerable reaction between the fiber and matrix. The SEM micrographs in Figure 10 further substantiate the degree of reaction in the oxidized-matrix composite. The fiber pullout surface is decorated with small, protruding nodules. These nodules, although less prevalent, were also found on the *standard*-matrix composite; but none could be found in the *reduced*-matrix composite. It seems likely that these modules contribute to the low strength and limited fiber pull-out in the *oxidized*- and *standard*-matrix composites. The nodules appear to be hollow gas bubbles.

Together with the model presented in the last section, these observations suggest that an extensive interface reaction has occurred, and has been consumed through internal oxidation and gas generation. In the *reduced*-matrix composite, these was sufficient oxygen activity to create the carbon interphase, but oxygen depletion near the interface limited any further oxidation. In the *oxidized*-matrix composite, the oxygen activity was sufficiently high to consume carbon faster than it could be created. Altogether, these experimental data show the importance of oxygen activity in the matrix during fabrication - even though the fabrication is performed in an inert environment. In glasses with variable valence oxides (e.g., As_2O_5/As_2O_3) or impurities (e.g., Fe_2O_3/FeO or H_2O/H_2), the effects can be more dramatic.

SUMMARY

It has been shown that the oxygen potential of glass is a useful parameter for defining the driving force for reaction with non-oxide reinforcement phases such as silicon-carbide. The ability to calculate these potentials using the concept of

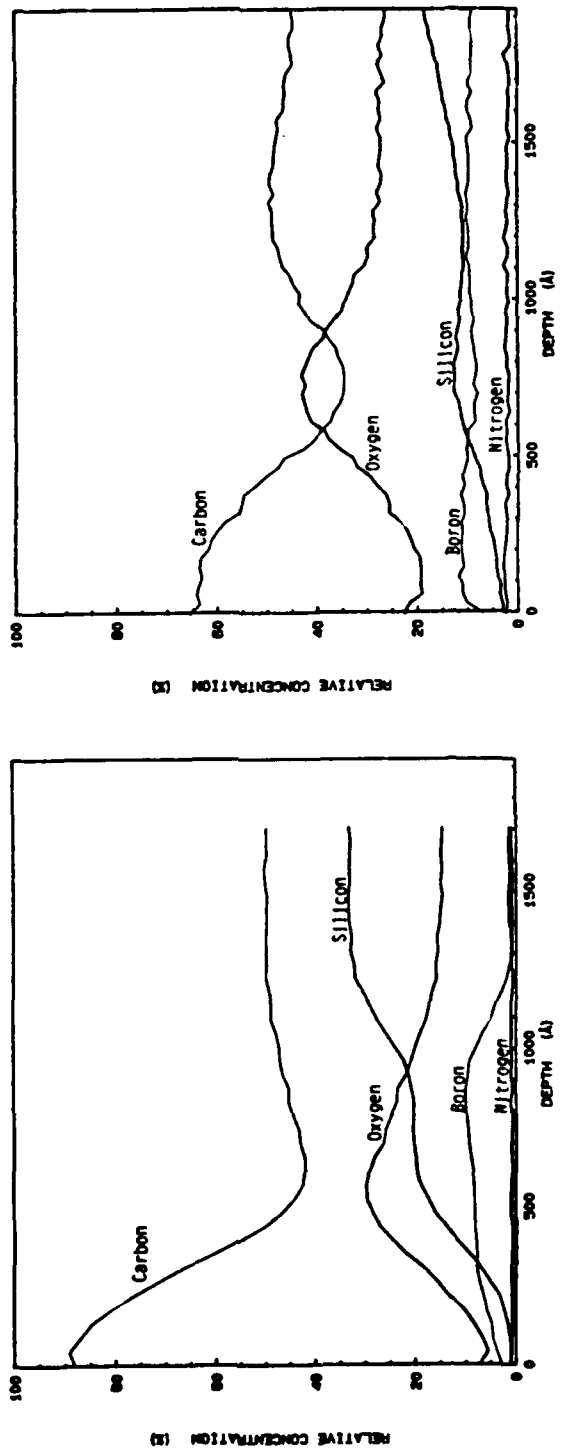

Figure 9. Auger depth profiles of NiCALON fiber pullouts; the glass matrix phases used to fabricate these composites were initially melted under (a) reducing conditions, or (b) oxidizing conditions.

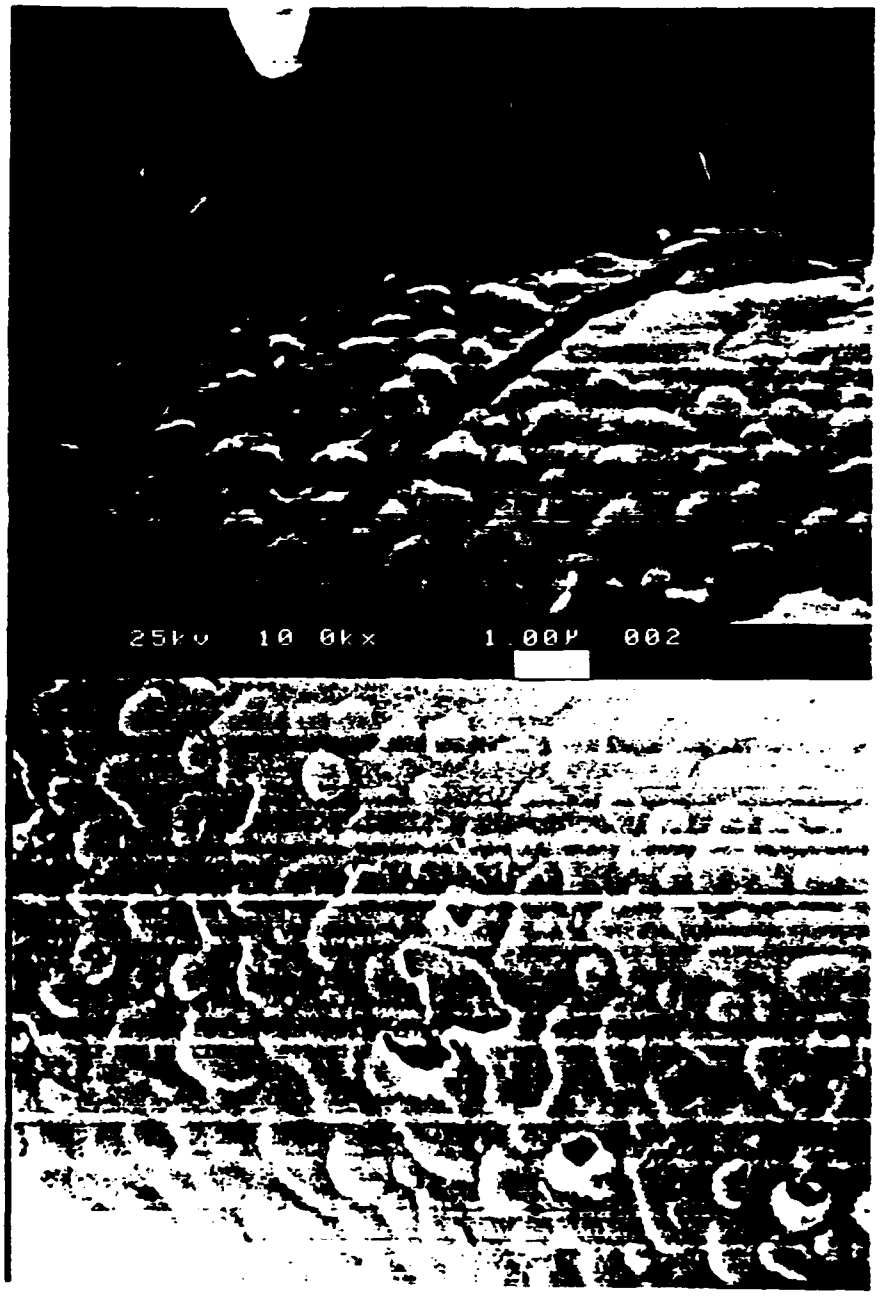

Figure 10. SEM micrographs of the NiCALON fiber pullouts on the *oxidized*-matrix composite fracture surface.

liquid associate species is significant because the direct measurement of the oxygen potential of glass is difficult. The calculations reveal that the presence and concentration of easily reduced metal oxides in the glass will determine the extent of this reaction. They also reveal that the melting history of a glass matrix precursor (or more specifically, the oxygen potential during quenching of the glass frit) can influence the interface reactions that occur during subsequent fabrication or use of the composite in a non-oxidizing atmosphere. These effects of glass composition and processing can be used to control the interface reactions. At the same time, they explain why the processing and performance of glass-matrix composites depend upon so many factors, and in many cases, are not reproduced. Some of the most common impurities in glass, and the typical methods of glass processing, can dramatically and unknowingly influence these parameters. The transient nature of the carbon interphase, and its dependence upon these parameters, explains many of the variations reported in the literature (1-4, 7-10) for composite performance and interface microstructure in SiC/glass systems.

Fortunately, the thermochemical calculations — which have been verified here and elsewhere (14) — provide a convenient approach for making predictions and for guiding the design and application of composites. Unfortunately, the basic thermodynamic and transport properties necessary to further refine these approaches are lacking. The thermodynamic properties of polymer-processed fibers are most certainly very different than the properties of stoichiometric SiC; these data are now becoming available (15). Likewise, transport properties associated with reaction products at interfaces must be better established. This transport can influence the attainment of local equilibrium at interfaces, and thereby, promote or limit continued reaction. Altogether, one concludes that thermochemical modeling is best used in combination with experimental observations at real interfaces. In this way, the most important parameters and effects can be determined even in the absence of a complete thermodynamic or kinetic description. In the end, the most useful and realistic model will emerge.

ACKNOWLEDGEMENTS

The authors gratefully acknowledge the financial support of the Office of Naval Research (N00014-90-J-1392; Steve Fishman - Contract Monitor). We also thank Corning Inc., for their preparation of the special glassmelts and composites, and Jim Hoenigman for his expertise in the Auger analyses.

REFERENCES

1. J. J. Brennan, "Interfacial Characterization of Glass and Glass-Ceramic Matrix/Nicalon SiC Fiber Composites," pp. 546-560 in Proc. of the Conf. on Tailoring Multiphase and Composite Ceramics. Edited by R. E. Tressler, G. L. Messing, C. G. Pantano and R. E. Newnham. Plenum Press, New York, 1986.

2. H. C. Cao, E. Bischoff, O. Sbaizero, M. Rühle, A. G. Evans, D. Marshall and J. J. Brennan, "Effect of Interfaces on the Properties of Fiber-Reinforced Ceramics," *J. Am. Ceram. Soc.*, **73** [6], 1691-99 (1990).

3. F. Lin. T. Marieb, A. Morrone and S. Nutt, "Thermal Oxidation of Al_2O_3-SiC Whisker Composites: Mechanisms and Kinetics," Mat. Res. Soc. Symp. Proc., **120**, 323-332 (1988).

4. A. Jha and M. D. Moore, "A Study of the Interface Between Silicon Carbide Fibre and Lithium Aluminosilicate Glass Ceramic Matrix", Glass Techn., **33**, [1], 30-37 (1992).

5. K. Luthra, "Chemical Interactions in High-Temperature Ceramic Composites," *J. Am. Ceram. Soc.*, **71** [12], 1114-20 (1988).

6. N. S. Jacobson, K. N. Lee, and D. S. Fox, "Reactions of Silicon Carbide and Silicon (IV) Oxide at Elevated Temperatures," *J. Am. Ceram. Soc.*, **75** [6], 1603-1611 (1992).

7. L. A. Bonney and R. F. Cooper, ""Reaction-Layer Interfaces in SiC-Fiber-Reinforced Glass-Ceramics: A High-Resolution Scanning Transmission Electron Microscopy Analysis," *J. Am. Ceram. Soc.*, **73** [10], 2915-21 (1990).

8. M. Lancin, "Relationship between the Microstructure of the Interface and the Mechanical Behavior of Composites Materials," *J. Phys. III*, **1** [6] 1141-1166 (1991).

9. R. Chaim, and A. Heuer, "Carbon Interfacial Layers Formed by Oxidation of SiC in SiC/Ba-Stuffed Cordierite Glass-Ceramic Reaction Couples," *J. Am. Ceram. Soc.*, **74** [7], 1663-67 (1991).

10. J. J. Brennan and S. R. Nutt, "SiC-Whisker-Reinforced Glass-Ceramic Composites: Interfaces and Properties", *J. Am. Ceram. Soc.*, **75** [5], 1205-1216 (1992).

11. D. W. Bonnell and J. W. Hastie, "A Predictive Thermodynamic Model for Complex High Temperature Solution Phases XI," in Materials Chemistry at High Temperatures - Vol 1. Edited by Hastie Humana Press, 1990, pp 313-334.

12. P. M. Benson, K. E. Spear and C. G. Pantano, "Thermochemical Analyses of Interface Reactions in Carbon-Fiber Reinforced Glass Matrix Composites," in Ceramic Microstructures '86. Edited by Pask and Evans. Plenum Publishing Corporation, 1988, pp 415-425.

13. G. Eriksson and K. Hack, "ChemSage," Edition 2.1.1 Oct. 1991, GTT MbH, Mies-Van Der Rohe Str. 25, 5110 Aachen, Germany.

14. G. Qi, K. E. Spear and C. G. Pantano, "Carbon-Layer Formation at Silicon-Carbide Glass Interfaces", Materials Science and Engineering, 1993 (to appear).

15. P. Rocabois, C. Chatillon, C. Bernard, "Mass Spectrometry Experimental Investigation and Thermodynamic Calculation of the Si-C-OSystem and Si_x-C_y-O_z Fibre Stability," to be presented at HT-CMC93, ECCM6, (1993).